

# Liver Motion Estimation via Locally Adaptive Over-Segmentation Regularization

Bartłomiej W. Papież<sup>1</sup>, Jamie Franklin<sup>2</sup>, Mattias P. Heinrich<sup>4</sup>,  
Fergus V. Gleeson<sup>3</sup>, and Julia A. Schnabel<sup>1</sup>

<sup>1</sup> Institute of Biomedical Engineering,  
Department of Engineering Science, University of Oxford, UK  
`bartlomiej.papiez@eng.ox.ac.uk`

<sup>2</sup> Department of Oncology, University of Oxford, UK

<sup>3</sup> Department of Radiology, Churchill Hospital,  
Oxford University Hospitals NHS Trust, Oxford, UK

<sup>4</sup> Institute of Medical Informatics, University of Lübeck, Germany

**Abstract.** Despite significant advances in the development of deformable registration methods, motion correction of deformable organs such as the liver remain a challenging task. This is due to not only low contrast in liver imaging, but also due to the particularly complex motion between scans primarily owing to patient breathing. In this paper, we address abdominal motion estimation using a novel regularization model that is advancing the state-of-the-art in liver registration in terms of accuracy. We propose a novel regularization of the deformation field based on spatially adaptive over-segmentation, to better model the physiological motion of the abdomen. Our quantitative analysis of abdominal Computed Tomography and dynamic contrast-enhanced Magnetic Resonance Imaging scans show a significant improvement over the state-of-the-art Demons approaches. This work also demonstrates the feasibility of segmentation-free registration between clinical scans that can inherently preserve sliding motion at the lung and liver boundary interfaces.

## 1 Introduction

Analysis of functional abdominal imaging (e.g. dynamic magnetic resonance imaging (DCE-MRI)) and structural imaging (such as CT or MRI) is an emerging research area that can potentially lead to improved strategies for differential diagnosis and planning of personalized treatment (e.g. patient stratification) of abdominal cancer. In this work, we present a generic approach for intra-subject motion correction of time sequences, applied to both standard 4D CT acquisition, and relatively new quantitative imaging techniques such as DCE-MRI. This will ultimately provide new opportunities for tumor heterogeneity assessment for patients, with the potential of extending our understanding of human liver tumor complexity [10]. Deformable registration of time scans acquired using modalities with contrast agent is challenging due to: 1) significant amount of motion between consecutive scans including sliding motion at the lung and liver

interface; 2) low contrast of liver tissue; and 3) local volume intensity changes due to either contrast uptake in DCE-MRI. Thus, robust image registration is an inevitable post-acquisition step to enable quantitative pharmacokinetic analysis of motion-free DCE-MRI data.

Conventional motion correction algorithms use generic similarity measures such as sum-of-squared differences with a statistical prior to find an optimal transformation [5]. Alternatively, registration can be performed using a physiological image formation model [3]. However in both cases, the estimated transformation is highly influenced by the chosen regularization model. In the classic Demons framework, the diffusion regularization is performed by Gaussian smoothing of the estimated deformation field [14] that generates a smooth displacement field. However, the complex physiology of abdominal motion during breathing involves modeling of the liver sliding at the thoracic cage, which has been addressed by only a few registration algorithms [15,16,11]. Limitations of the aforementioned motion correction methods include the need for segmenting the liver surface [15,16,11]. Moreover, hepatic deformations [4] that is secondary to breathing has not been analyzed in motion models proposed so far.

In this paper, we propose a novel registration approach, referred to as SLIC Demons, owing to the use of the Simple Linear Iterative Clustering algorithm [1] for a liver motion estimation model. This model is used then for an accurate deformable registration of DCE-MRI data to enforce the plausibility of the estimated deformation field, e.g. preservation of sliding motion at the thoracic cage and at the lung boundaries whilst not requiring any prior liver segmentation. The contributions of this work are as follows. First, we introduce an accurate model for the regularization of the deformation field, which incorporates additional (anatomical) information from so-called *guidance* images in a computationally efficient manner. This regularization is embedded in a classic non-rigid Demons registration framework using the local correlation coefficient [9] as a similarity measure to handle local intensity changes due to contrast uptake. The improved performance on a publicly available liver CT data [11] is demonstrated. Finally, the robustness of the method on a challenging clinical application of DCE-MRI liver motion compensation is quantitatively assessed.

## 2 Methodology

**Deformable Image Registration.** In the classic formulation [8], deformable image registration is defined as a global energy minimization problem with respect to the geometrical transformation describing the correspondences between input images  $I_F$  and  $I_M$ :

$$\hat{\mathbf{u}} = \arg \min_{\mathbf{u}} (Sim(I_F, I_M(\mathbf{u})) + \alpha Reg(\mathbf{u})) \quad (1)$$

where  $\hat{\mathbf{u}}$  is the optimal displacement field,  $Sim$  is a similarity measure,  $Reg$  is a regularization term, and  $\alpha > 0$  is a weighting parameter. The Demons framework [14], due to its simplicity and efficiency, is a common choice to solve Eq. (1)



**Fig. 1.** Corresponding region of interest (axial view of the segmental branch of hepatic artery) selected by the expert from consecutive volumes of DCE-MRI sequence. Besides intensity changes caused by the contrast agent, local structures are visibly correlated, which is also confirmed by quantitative evaluation of LCC Demons.

when sum-of-squared differences (or any other point-wise difference metric) is used as a similarity measure, and a diffusion model is used for regularization. For the Demons framework, the optimization procedure alternates between minimizing the energy related to the similarity  $Sim$  and the regularization  $Reg$  in an iterative manner. In this work, due to the low contrast of the liver in CT, and change of intensity values owing to the contrast uptake between consecutive DCE-MRI volumes (see an example in Fig. 1), we propose to use the local correlation coefficient (LCC) as a similarity measure. This is further motivated by recent work that used LCC-Demons for brain MRI registration due to their independence of any additive and multiplicative bias in the data [9].

**Filtering of the Deformation Field.** Accurate alignment of intra-subject dynamic imaging data is challenging not only because of intensity changes due to contrast uptake, but also due to the complexity of motion to be estimated. In the Demons framework, diffusion regularization is performed by Gaussian smoothing of the estimated deformation field. However, the complex physiology of respiratory motion involves more than just modeling of the liver sliding at the thoracic wall [11,12]. The human liver is non-uniform in composition as it is built of vascular structures and filamentous tissue. Hence it is not adequate to model hepatic motion by performing segmentation of the whole liver prior to registration [15,16]. Thus, inspired by a previous approach of spatially adaptive filtering of the deformation field [13,12], and the guided image filtering technique developed for computer vision applications [6], we present a generic approach for regularization. In our approach, the estimated deformation field is spatially filtered by considering the context of the guidance information coming either from one of the input images itself or another auxiliary image (e.g. from a segmentation mask). The output deformation field  $\mathbf{u}_{out}$  of the guided image filtering technique of the input deformation field  $\mathbf{u}_{in}$  is based on a linear model of the guidance image  $I_G$  in the local neighborhood  $\mathcal{N}$  centered at the spatial position  $\mathbf{x}$ , and is defined as follows [6]:

$$\mathbf{u}_{out}(\mathbf{x}) = \sum_{\mathbf{y} \in \mathcal{N}} W_{\mathbf{y}}(I_G) \mathbf{u}_{in}(\mathbf{y}) \quad (2)$$

where  $W_{\mathbf{y}}$  is a filter kernel derived from the guidance image  $I_G$ . An example of such local filter kernel weights  $W_{\mathbf{y}}$  are the bilateral filtering kernels proposed by [12].

Note that a guided image filter can be implemented using a sequence of box filters making the computing time independent of the filter size [6].

**Guidance for Accurate Modeling of Complex Liver Motion.** An additional motivation for using the guided filter technique is that it allows incorporation of prior knowledge for deformation field regularization. For example, the output deformation field can be filtered with respect to the registered image (*self-guidance*), or labels obtained from segmentation of the entire thoracic cage. While the use of masks in [15,16] is limited to just a few objects, multi-object segmentation can be easily added to the presented approach by using a multi-channel guidance image (e.g. similarly to the channels in an RGB image) without a significant increase of computational complexity [6]. Therefore, we consider an alternative guidance image, which is built based on the concept of sparse image representation based on supervoxel clustering. Following [7], we adapt Simple Linear Iterative Clustering (SLIC) [1] for supervoxel clustering. SLIC performs an image segmentation that corresponds to spatial proximity (spatial compactness) and image boundaries (color similarity). SLIC is designed to generate  $K$  approximately equally-sized supervoxels. The Euclidean distance between voxel  $\mathbf{x}$  and a cluster center  $\mathbf{y}$  is calculated as  $d_{\mathbf{xy}} = \|\mathbf{x} - \mathbf{y}\|$  and the distance measuring the gray-color proximity is given by:  $d_I = \sqrt{(I(\mathbf{x}) - I(\mathbf{y}))^2}$ . The combination of the two normalized distances  $d_{\mathbf{xy}}$  and  $d_I$  is defined in the following way:  $D = \sqrt{(d_{\mathbf{xy}}/S)^2 + (d_I/m)^2}$  where  $m$  is a parameter determining the relative importance between color and spatial proximity. A larger value of  $m$  results in supervoxels with more compact shapes, whereas for small  $m$  the resulting clusters have less regular shapes and sizes, but they are more adapted to image details and intensity edges. The parameter  $S = \sqrt[3]{N/K}$  corresponds to the sampling interval of the initial spacing of the cluster centers. The algorithm starts from a set of equally spaced cluster centers. After each iteration the cluster centers are recomputed, and the algorithm is iterated until the convergence.

Because SLIC performs an image segmentation that corresponds to spatial and intensity proximity, it removes the redundant intensity information of voxels in the homogeneous regions. However, such clustering becomes also very inconsistent in such regions. In the context of filtering the deformation field during registration, this is a major drawback, because filtering with respect to the clustered image would introduce artificial discontinuities. This is called over-segmentation, and it is a common problem for simple image-driven regularization models. In [7] the authors proposed to use multiple channel (layers) of supervoxels to obtain a piecewise smooth deformation model. To generate such different channels of supervoxels, the SLIC algorithm was run several times with randomly perturbed initial cluster centers. Image clustering in homogeneous regions will result in different clusters for each channel. However, image regions with sufficient structural content will not be affected by random perturbation of SLIC cluster centers. Furthermore, the displacement fields obtained for each channel separately can be averaged to construct the final displacement field, and therefore avoid discontinuities in homogeneous regions [7]. In our case, we can

use each channel of supervoxels  $S$  as a separate channel of our guidance image  $I_G = [S_1, S_2, \dots, S_N]$  and then perform an efficient filtering of the deformation field with respect to such multichannel guidance image.

For a given  $I_G$ , the weights  $W_{GIF}$  of the guided filter at the position  $\mathbf{x}$  are explicitly expressed in the following way:

$$W_{GIF}(I_G) = 1 + (I_G - \mu_{I_G})^T (\Sigma_{I_G} + \varepsilon \mathbf{U})^{-1} (I_G - \mu_{I_G}) \quad (3)$$

where  $\mu_{I_G}$  and  $\Sigma_{I_G}$  are the mean and covariance of the guidance image  $I_G$  in the local neighborhood  $\mathcal{N}$ , and  $\mathbf{U}$  denotes the identity matrix. It has been shown [6] that in the case of the guidance image  $I_G$  being a multichannel image, the weights of the guided filter (defined in Eq. (3)) can be computed without a significant increase of computational complexity compared to single-channel image guidance (however for  $N$  numbers of channels, inversion of an  $N \times N$  matrix is required for each voxel). The SLIC [1] algorithm is reported to have a linear complexity with respect to the number of image voxels and therefore is easily applicable to large medical data sets. It is also important to note that the SLIC algorithm is memory efficient when dealing with large volumes (see more details [1]). Our implementation of SLIC is based on jSLIC<sup>1</sup>.

**Physiological Plausibility.** The estimated sliding motion should have three properties: 1) Motion normal to the organ boundary should be smooth both across organ boundaries and within organs, 2) Motion tangential to the organ boundary should be smooth in the tangential direction within each individual organ, and 3) Motion tangential to the organ boundary is not required to be smooth across organ boundaries [11]. The presented regularization model addresses explicitly 2) and 3), while diffeomorphic formulation of the overall registration [9] prevents folding between organs. Furthermore, filtering the deformation field using a guided filter, which is derived from a locally linear model, provides an invertibility constraint (due to the log-Euclidean parameterization [2]).

### 3 Evaluation and Results

We performed deformable registration using diffeomorphic logDemons with a symmetric local correlation coefficient (LCC) as a similarity criterion [9]. We use the following parameter settings for the optimization: three multi-resolution levels, and a maximum number of iterations of 50. For liver CT data, we empirically determined the LCC smoothing parameter  $\sigma_{LCC}=2$  the regularization parameter  $\sigma = 3$  for LCC-Demons, a filter radius  $r=5$  and a regularization parameter  $\alpha=0.1$  was found to give the best results for the SLIC Demons. For registration of DCE-MRI, we employ a larger patch  $\sigma_{LCC}=5$  to calculate the local correlation coefficient, while the other parameters remain the same. It is worth noting that the parameters for the SLIC Demons have a low sensitivity, causing an increase of Target Registration Error (TRE) of only 0.1mm when changing  $r$  between 4

<sup>1</sup> jSLIC: superpixels in ImageJ, [http://fiji.sc/CMP-BIA\\_tools](http://fiji.sc/CMP-BIA_tools)

and 6, and  $\alpha$  between 0.2 and 0.01. For SLIC, the weighting parameter  $m=20$  was selected empirically (for intensity range between 0 - 255). We found that three channels of the SLIC guidance image provides satisfactory results, and further increasing the number of channels does not improve the overall TRE significantly.

**Results on 4DCT.** For the quantitative evaluation of liver motion, the SLIC Demons are tested on volumes of abdominal 4D-CT data sets that are publicly available. Four inhale and exhale abdominal CT image pairs were obtained from the Children’s National Medical Center/Stanford<sup>2</sup> that were previously used for validation purposes in [11]. Following preprocessing steps performed in [11], the volumes were cropped, thresholded, intensity-normalized, and finally linearly resampled to isotropic spacing of  $2\text{mm}^3$ . To quantify the registration accuracy, the TRE was calculated for the well-distributed set of landmarks, which are provided with this data set ( $\approx 50$  landmarks per case for lungs, and  $\approx 20$  landmarks per case for the abdomen including liver). For all cases in this data set, the end-of-inspiration volume was chosen as a reference, and the end-of-expiration volume as a moving image. The initial average TRE is  $7.04 \pm 4.3\text{mm}$  for lung landmarks, and  $6.44 \pm 3.4\text{mm}$  for abdominal landmarks. A significantly lower TRE (p-value $<0.05$  using a two-sample Wilcoxon rank sum test) is obtained by deformation fields estimated using the framework based on the guided filtering of deformation fields (TRE= $2.08\text{mm}$  for lungs and TRE= $2.19\text{mm}$  for abdomen) when compared to the classic Demons (TRE= $3.24\text{mm}$  for lungs and = $2.5\text{mm}$  for abdomen). All resulting deformation fields are invertible within the region of interest (indicated by the positive value of the Jacobian). Moreover, the TRE yielded by the proposed method is lower than the best results reported so far in the literature ( $2.15\text{mm}$  for lungs and  $2.56\text{mm}$  for abdomen [11]). Employing registration with guidance for regularization of the deformation field preserves discontinuities at the pleural boundaries whilst satisfying smoothness requirements inside the lungs and liver (e.g. the difference between the estimated deformation fields close to the lung boundaries shown in Fig. 2).

**Results on DCE-MRI.** The presented registration approach was additionally applied for two abdominal DCE-MRI sequences acquired at the Churchill Hospital in Oxford as a part of an ongoing clinical trial exploring the feasibility of novel imaging techniques to assess how tumors are responding to treatment. The DCE-MRI data were acquired with a variable time, yielding 25 volumes with the volume resolution of  $0.78 \times 0.78 \times 2.5\text{mm}$ . The initial average TRE is  $15.82\text{mm} \pm 8.5$  for the landmarks annotated within the liver region. Similarly as for the previous experiment on the 4D liver CT, a significantly lower TRE (p-value $<0.05$  using a two-sample Wilcoxon rank sum test) was obtained using the framework based on the guided filtering of deformation fields (TRE= $2.3\text{mm} \pm 0.9$  for the liver) when compared to the classic Demons (TRE= $2.7\text{mm} \pm 1.7$  for the liver). The results of this evaluation indicate that the proposed spatially adaptive

---

<sup>2</sup> MIDAS Community: 4D CT Liver with segmentations

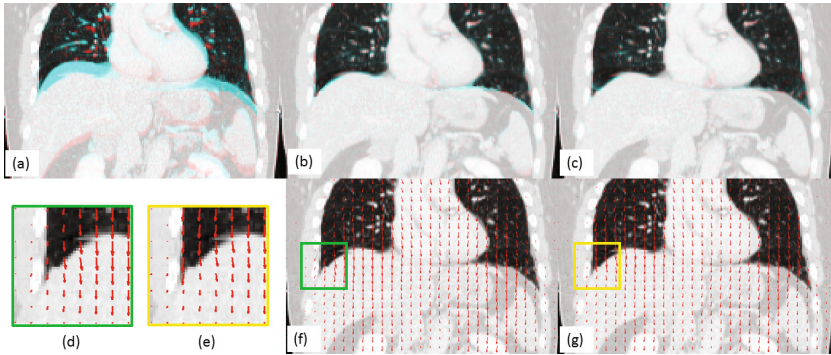


**Fig. 2.** Coronal view of 3D deformable CT/CT registration results. Color-coded intensity differences between image pair: (a) before registration, using (b) Demons, and (c) SLIC Demons. The estimated deformation field depicted: using (f) Demons, and (g) SLIC Demons with the corresponding zoomed images of the region of interest (labeled by box in the bottom row). Registration with SLIC yields a smooth deformation field inside the liver, while capturing the sliding motion across the pleural cavity boundaries.

regularization is capable of handling complex hepatic motion that is naturally present during DCE-MRI acquisition of the liver.

## 4 Discussion and Conclusions

We have presented an automated regularization approach for deformable registration that enables estimation of physiologically plausible hepatic deformations. For this purpose, the classic diffusion regularization using Gaussian smoothing was replaced by a fast image guidance technique that filters the estimated deformation field with respect to the anatomical tissue properties directly derived from the guidance image. The presented approach forms a spatially adaptive regularization that is capable of accurately preserving discontinuities that naturally occur between the lungs, liver and the pleura. We verified the robustness of our method on a publicly available data set [11], for which the results clearly demonstrated its advantages in terms of accuracy and computational efficiency when compared to the state-of-the-art methods. The computation time per registration using the presented framework is  $\approx 5$  mins per 3D pair (a standard CPU, with a non-optimized C++ code), and is several times faster compared to the bilateral filtering procedure proposed in [12]. We also applied our proposed method to an on-going clinical trial, where patients are scanned with DCE-MRI, and for which we obtained a good visual alignment of the data. The presented technique has the potential to generalize to other modalities and clinical applications in which compensation of the complex motion is essential.

**Acknowledgments.** We would like to acknowledge funding from the CRUK/EPSRC Oxford Cancer Imaging Centre. BWP would like to thank D.F. Pace for providing the additional 4D liver CT patient annotations.

## References

1. Achanta, R., Shaji, A., Smith, K., Lucchi, A., Fua, P., Süsstrunk, S.: SLIC Superpixels compared to state-of-the-art superpixel methods. *IEEE Trans. Pattern Anal. Mach. Intell.* 34(11), 2274–2282 (2012)
2. Arsigny, V., Commowick, O., Pennec, X., Ayache, N.: A log-Euclidean framework for statistics on diffeomorphisms. In: Larsen, R., Nielsen, M., Sporring, J. (eds.) *MICCAI 2006*. LNCS, vol. 4190, pp. 924–931. Springer, Heidelberg (2006)
3. Bhushan, M., Schnabel, J.A., Risser, L., Heinrich, M.P., Brady, J.M., Jenkinson, M.: Motion correction and parameter estimation in dceMRI sequences: application to colorectal cancer. In: Fichtinger, G., Martel, A., Peters, T. (eds.) *MICCAI 2011, Part I*. LNCS, vol. 6891, pp. 476–483. Springer, Heidelberg (2011)
4. Clifford, M.A., Banovac, F., Levy, E., Cleary, K.: Assessment of hepatic motion secondary to respiration for computer assisted interventions. *Comput. Aided Surg.* 7(5), 291–299 (2002)
5. Hamy, V., Dikaios, N., Punwani, S., Melbourne, A., Latifoltojar, A., et al.: Respiratory motion correction in dynamic MRI using robust data decomposition registration—Application to dce-MRI. *Med. Image Anal.* 18(2), 301–313 (2014)
6. He, K., Sun, J., Tang, X.: Guided image filtering. *IEEE Trans. Pattern Anal. Mach. Intell.* 35(6), 1397–1409 (2013)
7. Heinrich, M.P., Jenkinson, M., Papież, B.W., Glesson, F.V., Brady, M., Schnabel, J.A.: Edge- and detail-preserving sparse image representations for deformable registration of chest MRI and CT volumes. In: Gee, J.C., Joshi, S., Pohl, K.M., Wells, W.M., Zöllei, L. (eds.) *IPMI 2013*. LNCS, vol. 7917, pp. 463–474. Springer, Heidelberg (2013)
8. Hermosillo, G., Chéfd’Hotel, C., Faugeras, O.D.: Variational methods for multimodal image matching. *Int. J. Comput. Vision* 50, 329–343 (2002)
9. Lorenzi, M., Ayache, N., Frisoni, G., Pennec, X.: LCC-Demons: a robust and accurate symmetric diffeomorphic registration algorithm. *Neuroimage* 81, 470 (2013)
10. Mescam, M., Kretowski, M., Bezy-Wendling, J.: Multiscale model of liver dce-MRI towards a better understanding of tumor complexity. *IEEE Trans. Med. Imag.* 29(3), 699–707 (2010)
11. Pace, D.F., Aylward, S.R., Niethammer, M.: A locally adaptive regularization based on anisotropic diffusion for deformable image registration of sliding organs. *IEEE Trans. Med. Imag.* 32(11), 2114–2126 (2013)
12. Papież, B.W., Heinrich, M.P., Fehrenbach, J., Risser, L., Schnabel, J.A.: An implicit sliding-motion preserving regularisation via bilateral filtering for deformable image registration. *Med. Image Anal.* 18(8), 1299–1311 (2014)
13. Staring, M., Klein, S., Pluim, J.P.W.: Nonrigid registration with tissue-dependent filtering of the deformation field. *Phys. Med. Biol.* 52, 6879–6892 (2007)
14. Vercauteren, T., Pennec, X., Perchant, A., Ayache, N.: Diffeomorphic Demons: Efficient non-parametric image registration. *NeuroImage* 45, S61–S72 (2009)
15. Wu, Z., Rietzel, E., Boldea, V., Sarrut, D., Sharp, G.C.: Evaluation of deformable registration of patient lung 4DCT with subanatomical region segmentations. *Med. Phys.* 35(2), 775–781 (2008)
16. Xie, Y., Chao, M., Xiong, G.: Deformable image registration of liver with consideration of lung sliding motion. *Med. Phys.* 38(10), 5351–5361 (2011)